

# A Raman spectroscopic study of the Mapungubwe oblates: glass trade beads excavated at an Iron Age archaeological site in South Africa

Linda C. Prinsloo<sup>1\*</sup> and Philippe Colomban<sup>1,2</sup>

<sup>1</sup> Department of Physics, University of Pretoria, Pretoria, South Africa

<sup>2</sup> Laboratoire Dynamique, Interactions et Réactivité (LADIR), UMR 7075 CNRS-Université Pierre et Marie Curie, 2 rue Henry Dunant, 94320 Thiais, France

Received 22 December 2006; Accepted 23 April 2007

Oblate seed beads (2–4 mm) excavated on Mapungubwe hill, an Iron Age site in South Africa, were analysed with Raman microscopy and supportive techniques to determine the glass technology and pigments used to produce the beads. The Raman spectra and XRF analysis of the beads classify the glass as a typical soda/lime/potash glass similar to Islamic glass from the 8th century (Ommayad), but with higher levels of aluminium, iron and magnesium. The turquoise, bright green, bright yellow and orange colours were obtained by utilizing a combination of cassiterite ( $\text{SnO}_2$ ) and lead tin yellow type II ( $\text{PbSn}_{1-x}\text{Si}_x\text{O}_3$ ). Doping with cobalt and manganese produced dark blue and plum-coloured beads. The Fe-S chromophore was detected through its resonance-enhanced spectrum in the black beads. Corrosion of the black beads was investigated and an organic phase detected on the beads, which might have influenced the corrosion process. This detailed profile of the glass technology used to produce the Mapungubwe oblates might eventually help to determine their provenance. Copyright © 2007 John Wiley & Sons, Ltd.

**KEYWORDS:** ancient glass trade beads; pigment identification; Fe-S chromophore

## INTRODUCTION

In a recent study, the Raman spectra and XRF analysis of the glaze of Chinese celadon shards excavated on Mapungubwe Hill, an Iron Age site in South Africa, suggested that the shards were manufactured in a later century than the original classification.<sup>1</sup> In order to obtain supportive evidence for these results, which will have an impact on the chronology of the whole region, a Raman spectroscopic study of the glass trade beads, excavated at the same site was undertaken.

Mapungubwe is a small flat-topped sandstone plateau situated in the Limpopo valley close to the present-day borders of South Africa, Botswana and Zimbabwe. An ancient legend, suggesting certain death upon ascending the hill, helped to protect the last resting place of the rulers of a prehistoric African trade kingdom (~1000–1290 A.D.) for more than seven centuries until its discovery in 1933.<sup>2</sup>

Excavations on Mapungubwe hill during 1933–1940 exposed three 'royal' burials, in which gold funerary objects, gold beads and bangles were found together with imported

glass beads. The sheer volume of beads recovered is staggering; from one burial alone 26 037 glass beads were counted, of which 24 808 were black. In comparison, the total number of beads excavated at Great Zimbabwe is 400 and at Manda, an island port on the Kenyan coast, 1150.<sup>3,4</sup> This makes the collection of the Mapungubwe beads, with an excavation time span from a Stone Age culture at bedrock to the time when the site was permanently abandoned (currently believed to be 1280 A.D.), invaluable. Furthermore, the central position of Mapungubwe hill, situated at the confluence of the Limpopo and Shashe rivers, made it from the earliest time accessible through old camel caravan routes to Egypt and the Mediterranean trade, and via the Limpopo river to the monsoon-based African east coast trade reaching as far as China. Furthermore, trade along the African west coast was accessible via the interior through Botswana and Angola, where Portuguese mariners traded in beads from Europe 150 years before they rounded the Cape of Storms and also dominated the African east coast trade.

Previous studies of the beads proposed that they were made in India, medieval Venice or Fustat, the Fatimid capital of Islamic Egypt (900–1250 A.D.).<sup>5–14</sup> Of special interest is a large number of beads, known as the Mapungubwe oblates

\*Correspondence to: Linda C. Prinsloo, Department of Physics, University of Pretoria, Pretoria, South Africa.  
E-mail: linda.prinsloo@up.ac.za

(Fig. 1), which have been shown to differ in appearance and chemical composition from beads excavated at other sites along the African east coast.<sup>9,12–14</sup>

It has been established that Raman spectroscopy is an excellent and non-destructive method to characterize glasses and porcelain glazes, as many features about the production process of the glass are encapsulated within a Raman spectrum.<sup>15–19</sup> Furthermore, Raman spectroscopy has been shown to greatly contribute to the understanding of the corrosion processes in historic glasses.<sup>19–21</sup>

In this paper we record the first results of our study of glass trade beads excavated on Mapungubwe hill and compare it with those obtained from different production technologies used in the Antique, European, Mediterranean, Islamic and Asian worlds.<sup>17</sup> In time we hope to extend

our research to beads excavated at other inland sites such as Great Zimbabwe, sites along the African east and west coasts, as well as the heirloom beads of various African ethnic groups such as the Venda and Ndebele. In order to establish the provenance of these beads, comparison with beads excavated at possible sites of origin is of the utmost importance.

## EXPERIMENTAL

### Samples

Our first priority was to investigate the small seed beads (2–4 mm) excavated from the 'royal burials' on Mapungubwe hill and known as the Mapungubwe oblates. [Oblate beads have been reheated to the point at which the entire



**Figure 1.** (a) Mapungubwe oblates: from top to bottom: cobalt blue, orange, black, yellow, plum, turquoise and green. (b) Larger black beads. (c) Corroded black beads.

length of the bead has a smoothly rounded profile. Length must be less than diameter (from Ref. 13) (Fig. 1(a)). The brilliantly coloured beads (cobalt, blue, orange, black, yellow, plum turquoise and green) were manufactured by the drawn method, usually associated with mass-produced beads. The ends were reheated and the glass is of a good quality without large bubbles.

Mixed in between the huge number of black beads were larger black beads, some cylindrical shaped and some round or oblate (Fig. 1(b)). These were also included in the study, as well as two black glass samples from glass-making sites around the Indian Ocean, (Arikamedu, India, and Giribawa, Sri Lanka) for comparative purposes.

### Experimental techniques

A multichannel notch-filtered INFINITY spectrograph (Jobin-Yvon-Horiba SAS, Longjumeau, France) equipped with a Peltier-cooled CCD matrix was used to record Raman spectra using 532 nm and 633 nm as excitation wavelengths. Some spectra were recorded with an XY Raman spectrometer from Dilor (liquid-nitrogen-cooled CCD), using the 514.5 nm (Coherent Innova 90 Ar<sup>+</sup>-laser) and 568 nm (Spectra-Physics krypton laser) lines as exciting radiation. In both cases collection of the scattered light in the backscattering geometry was made through an Olympus confocal microscope with either a long distance  $\times 50$  or  $\times 100$  microscope objective. Optimum recording conditions were obtained by varying laser power ( $<10$  mW at sample), microscope objective and size of the confocal hole. A few spectra were also recorded in the macro configuration of a Dilor XY instrument with the 406.7 nm line of a Kr<sup>+</sup> laser.

Mid-infrared transmission spectra were recorded of powdered samples pressed into KBr pellets (1 mg sample/100 mg KBr) using a Bruker 113v Fourier transform infrared (FTIR) spectrometer. The resolution was  $2\text{ cm}^{-1}$  and 32 scans were signal-averaged in each interferogram.

The chemical composition of the Mapungubwe oblates was determined with X-ray fluorescence (XRF) spectroscopy. A Sufficient number of beads (60–80) of each colour were selected to cover the bottom of a liquid sample holder and introduced into the ARL 9400XP+ wavelength dispersive XRF spectrometer. Analyses were executed using the UniQuant 5 software program, specifying the weight and area of the sample. The software analyses for all elements between F and U and only elements above the detection limits are reported.

SEM-EDS was used to determine the elemental composition of individual beads. A Jeol 5800 LV scanning electron microscope combined with a Vantage EDS analytical system with an accelerating voltage of 20 kV was used. The beads were coated with a 10 nm gold coating to create conductive surfaces.

The OriginPro 7.5 peak-fitting module was used to fit Gaussian peaks to the Raman spectra according the method

previously described. A constraint of full width at half-maximum (FWHM) $<100$  was placed on all peaks, except for the Lorentzian peak defined at  $980\text{ cm}^{-1}$  with a fixed FWHM at  $20\text{ cm}^{-1}$  and previously assigned to the signature of calcium-rich 'crystalline' nanoprecipitates.

## RESULTS AND DISCUSSION

### Characterization of the Mapungubwe oblate glass

The Raman spectrum of the amorphous phase of a glass consists of two broad bands around  $500$  and  $1000\text{ cm}^{-1}$ . The band at  $\sim 500\text{ cm}^{-1}$  originates from the  $\nu_2$  bending vibrations of isolated  $\text{SiO}_4$  tetrahedra and the one at  $\sim 1000\text{ cm}^{-1}$  from the coupled  $\nu_1$  and  $\nu_3$  Si–O stretching vibrations. In highly connected tetrahedral structures the band representing the bending modes have a high Raman intensity, and in weakly connected tetrahedral units, as caused by the addition of fluxing (ionic) agents, the intensity of this band decreases and the band representing the stretching modes becomes more intense. The relationship between the Raman index of polymerization ( $I_p = A_{500}/A_{1000}$  with  $A$  being the area under the Raman band), the glass composition and the processing temperature is well documented.<sup>15–17</sup>

In Fig. 2 the spectra of the glass of the Mapungubwe oblates are presented and it is clear that the spectra have more or less the same shape. In order to make a

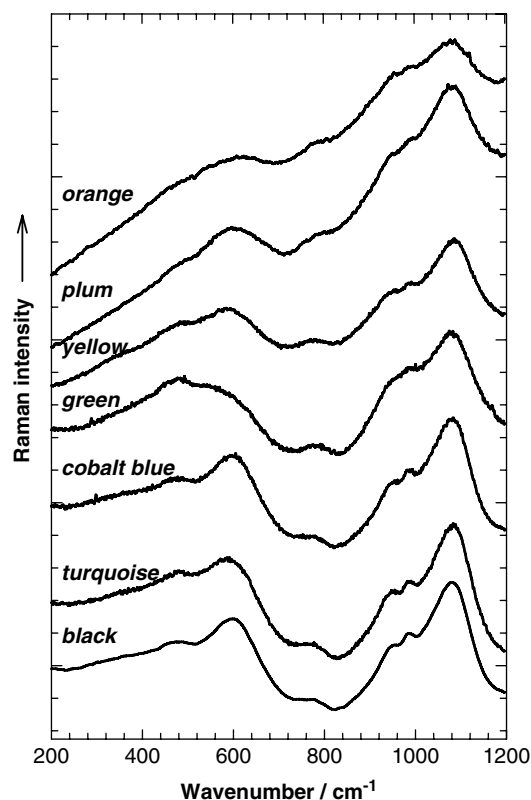


**Figure 2.** Raman spectra of the Mapungubwe oblates according to colour.

more detailed comparison between the spectra, a four-point baseline was subtracted from each spectrum as previously described.<sup>15–17</sup> The calculated polymerization index ( $I_p$ ) of all the colours glass ( $0.75 < I_p < 0.99$ ) classifies it as a typical soda/lime/potash glass, in the same category as Saljukids (11–13th century), Kutahya (17th century), Omayyads (8th century) or Phoenician/Roman glass.<sup>17</sup>

This is in agreement with the XRF results presented in Table 1A, which in Table 1B is reduced to the seven major oxides (normalized to 100% to remove the contribution of most pigments and other additives from the major glass composition), commonly used to facilitate the comparison between different glass types. It is very clear that the same basic glass recipe was used to produce all the beads ( $\text{SiO}_2 \sim 66\%$ ,  $\text{Na}_2\text{O} \sim 10\%$ ,  $\text{Al}_2\text{O}_3 \sim 9\%$ ,  $\text{CaO} \sim 5\%$ ,  $\text{K}_2\text{O} \sim 4\%$  and  $\text{MgO} \sim 3\%$ ).

The different components of the stretching envelope of porcelain glazes were assigned in the literature to silica vibrations with zero ( $Q^0$ ,  $800\text{--}850\text{ cm}^{-1}$ ), one ( $Q^1$ ,  $\sim 950\text{ cm}^{-1}$ ), two ( $Q^2$ ,  $\sim 1020\text{--}1040\text{ cm}^{-1}$ ), three ( $Q^3$ ,  $\sim 1100\text{ cm}^{-1}$ ) and four ( $Q^4$ ,  $\sim 1150\text{--}1250\text{ cm}^{-1}$ ) bridging oxygens per tetrahedral group. It has been shown that the position and relative ratio of the area under each peak can be used to differentiate further between closely related technologies and therefore a peak-fitting procedure (see 'Experimental Techniques') was

applied to all the spectra to extract these parameters for each glass colour.<sup>17</sup> The results are summarized in Table 2 and an example of the fitting procedure (yellow glass) is shown in Fig. 3. It is evident from the table that the Mapungubwe oblates form a clearly defined group with very similar Raman parameters in accordance with their related chemical compositions.

The envelope maxima of the Si–O stretches at  $\sim 1090\text{ cm}^{-1}$  for all the colours refines the classification according to the polymerization index to Omayyad glass from the 8th century and the basic glass recipe is part of group 3 (' $\text{Na}_2\text{O} + \text{K}_2\text{O} + \text{CaO}$ ' glass), as defined in Ref. 17. However, a closer look at Table 2 lifts out other differences between the Raman parameters, such as  $A\nu Q_2/A\nu Q_1 = 0.25$  for Omayyad glass, but  $0.60 < A\nu Q_2/A\nu Q_1 < 0.94$  for the Mapungubwe oblate glass and is therefore not an exact fit. This is verified by the compositional analysis of the glass (Table 1) as the Mapungubwe oblate glass has higher concentrations of aluminium, iron, magnesium and potassium than Omayyad glass<sup>17</sup>; this supports the continuous effort that is being made to increase the scope of the database.

## Pigments

The craft of colouring glass has been practiced since antiquity, although it was initially limited to essentially the blue and

**Table 1A.** XRF analysis of the Mapungubwe oblate beads

wt%	Black	Green	Yellow	Plum	Cobalt	Turquoise	Orange
$\text{SiO}_2$	61.71	58.90	56.34	60.96	65.46	61.99	53.57
$\text{Na}_2\text{O}$	10.36	8.54	9.44	11.44	10.14	9.84	8.17
$\text{Al}_2\text{O}_3$	8.97	7.52	7.57	8.43	8.22	8.58	7.9
$\text{CaO}$	6.24	4.30	3.78	5.11	4.72	4.38	4.03
$\text{K}_2\text{O}$	4.27	3.67	3.81	4.08	3.77	3.87	3.03
$\text{PbO}$	0.08	<sup>a</sup> 7.82	<sup>a</sup> 6.93	<sup>a</sup> 0.46	0.01	<sup>a</sup> 0.91	<sup>a</sup> 9.52
$\text{SnO}_2$	0.05	<sup>a</sup> 2.34	<sup>a</sup> 1.66	<sup>a</sup> 0.15	0.01	<sup>a</sup> 2.54	<sup>a</sup> 2.21
$\text{MgO}$	3.85	2.37	2.50	3.97	2.87	2.73	2.93
$\text{Fe}_2\text{O}_3$	1.50	1.53	1.48	1.54	<sup>a</sup> 2.08	1.59	1.28
$\text{Cl}$	0.95	0.53	0.71	0.60	0.67	0.73	0.51
$\text{P}_2\text{O}_5$	0.89	0.55	0.57	0.53	0.83	0.72	0.7
$\text{SO}_3$	<sup>a</sup> 0.31	0.18	<0.01	0.27	0.21	0.23	<0.01
$\text{Co}_3\text{O}_4$	<0.01	<0.01	<0.01	<0.01	<sup>a</sup> 0.17	0.01	0.01
$\text{TiO}_2$	0.25	0.26	0.31	0.25	0.27	0.29	0.24
$\text{S}$	<sup>a</sup> 0.10	<0.01	<0.01	<0.01	<0.01	<0.01	<0.01
$\text{CuO}$	0.10	<sup>a</sup> 1.04	0.05	0.03	0.01	<sup>a</sup> 1.23	0.08
$\text{BaO}$	0.10	0.08	<sup>a</sup> 0.24	0.14	0.10	0.09	<sup>a</sup> 0.20
$\text{MnO}$	0.08	0.07	<sup>a</sup> 0.37	<sup>a</sup> 1.80	0.06	0.06	<sup>a</sup> 0.54
$\text{As}_2\text{O}_3$	<0.01	<0.01	<0.01	<0.01	<sup>a</sup> 0.21	0.01	0.07
$\text{SrO}$	0.07	0.05	0.07	0.01	0.07	<0.01	0.06
$\text{ZrO}_2$	0.02	0.02	0.03	0.02	0.02	0.02	0.03
$\text{ZnO}$	0.02	<sup>a</sup> 0.13	0.04	0.05	0.02	0.05	<sup>a</sup> 0.72
$\text{U}_3\text{O}_8$	<0.01	<0.01	0.02	<0.01	<0.01	<0.01	0.03
$\text{NiO}$	<0.01	0.01	<0.01	<0.01	<0.01	0.01	0.02

<sup>a</sup> Chemicals used as pigments.

**Table 1B.** Normalised compositions of the seven major oxides of the Mapungubwe oblate beads

wt%	Black	Green	Yellow	Plum	Cobalt	Turquoise	Orange
SiO <sub>2</sub>	63.7	67.8	66.3	63.8	67.3	66.7	66.2
Na <sub>2</sub> O	10.7	9.8	11.1	12.0	10.4	10.6	10.1
Al <sub>2</sub> O <sub>3</sub>	9.3	8.7	8.9	8.8	8.5	9.2	9.8
CaO	6.4	5.0	4.7	5.3	4.9	4.7	5.0
K <sub>2</sub> O	4.4	4.2	4.5	4.3	3.9	4.2	3.7
MgO	<sup>a</sup> 4.0	2.7	2.9	<sup>a</sup> 4.2	3.0	2.9	3.7
Fe <sub>2</sub> O <sub>3</sub>	1.5	1.8	1.7	1.6	<sup>a</sup> 2.1	1.7	1.6

<sup>a</sup> Chemicals used as pigments.

**Table 2.** Main Raman parameters of the Mapungubwe oblates according to colour

Sample	<i>I<sub>p</sub></i>	$\nu$ Q <sub>0</sub>	$\nu$ Q <sub>1</sub>	$\nu$ Q <sub>2</sub>	$\nu$ Q <sub>3</sub>	$\nu$ Q <sub>4</sub>	<i>A<sub>v</sub></i> Q <sub>0</sub>	<i>A<sub>v</sub></i> Q <sub>1</sub>	<i>A<sub>v</sub></i> Q <sub>2</sub>	<i>A<sub>v</sub></i> Q <sub>3</sub>	<i>A<sub>v</sub></i> Q <sub>4</sub>	<i>A<sub>v</sub></i> Q <sub>2</sub> / <i>A<sub>v</sub></i> Q <sub>3</sub>	<i>A<sub>v</sub></i> Q <sub>2</sub> / <i>A<sub>v</sub></i> Q <sub>1</sub>
Black	0.83	781	949	1026	1083	1104	0.5	13.8	12.7	16.9	9.7	0.75	0.92
Green	0.75	785	953	1023	1083	1125	1.0	17.5	11.3	17.7	9.3	0.64	0.65
Yellow	0.78	783	944	1021	1089	1114	0.8	14.2	13.3	17.1	10.8	0.78	0.94
Plum	0.72	780	957	1037	1087	1129	0.5	19.6	11.7	20.0	5.5	0.60	0.60
Cobalt	0.80	785	961	1038	1089	1129	0.8	15.9	9.1	19.3	9.9	0.47	0.57
Turquoise	0.76	780	947	1026	1087	1114	0.7	14.6	12.2	18.2	10.4	0.67	0.84
Orange	0.74	784	953	1036	1091	1119	1.0	18.0	11.1	20.5	5.9	0.54	0.62

*I<sub>p</sub>*, index of polymerization; Q<sub>*n*</sub>, centre of gravity wavenumber (in cm<sup>-1</sup>) of the Si–O stretching Q<sub>*n*</sub> component; *A<sub>v</sub>*Q<sub>*n*</sub>, component area (% of the total peak area).

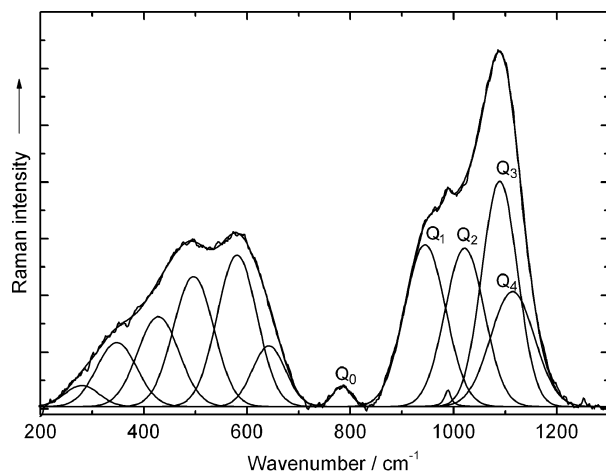


**Figure 3.** Example of the peak-fitting procedure applied to yellow glass.

green colours. The Mapungubwe oblates display a varied colour palette, indicating quite a high degree of chemical engineering competence, because colouring is dependent on the composition of the basic glass, as well as the nature and composition of the colouring substance.<sup>22</sup> The technology involved in colouring a glass and the pigments used may give an indication of where the glass was produced. Complicating the issue, though, is the fact that pigment ores (e.g. cobalt

ores), as well as glass cullet, were exported all over the world to secondary glass working sites.

The Raman spectra of the pigments/opacifiers used to obtain the Mapungubwe oblate colour palette (Fig. 1(a)) are presented in Fig. 4. Spectra of the pure pigments could be obtained from some samples by focussing the laser beam on small crystallites, which were visible within the glassy matrix using the ×100 objective of the microscope.

The well-known spectrum of the anatase phase of TiO<sub>2</sub> (Fig. 4(a)) was recorded on many of the beads and correlates with the XRF measurements (Table 1), which determined the presence of ~0.25% TiO<sub>2</sub> in all the glass beads under study. The rutile phase was not detected in any of the spectra. Although TiO<sub>2</sub> is not a pigment as such but an opacifier, its presence together with that of iron (present in all the samples, Table 1) can be used by varying the Fe:Ti ratio, firing temperature and oxidation conditions to obtain a large variety of differently coloured glasses as richly illustrated in the celadon glazes of Chinese potters.<sup>23</sup>

The turquoise, bright green, bright yellow and orange colours were obtained by utilizing a combination of cassiterite (SnO<sub>2</sub>) and lead tin yellow type II (PbSn<sub>1-x</sub>Si<sub>x</sub>O<sub>3</sub>). The very strong characteristic peak of cassiterite at 630 cm<sup>-1</sup> was observed in the Raman spectra of the bright green and turquoise beads (Fig. 4(b) and (c)) and the spectrum of lead tin yellow type II, with characteristic strong peak at 137 cm<sup>-1</sup>

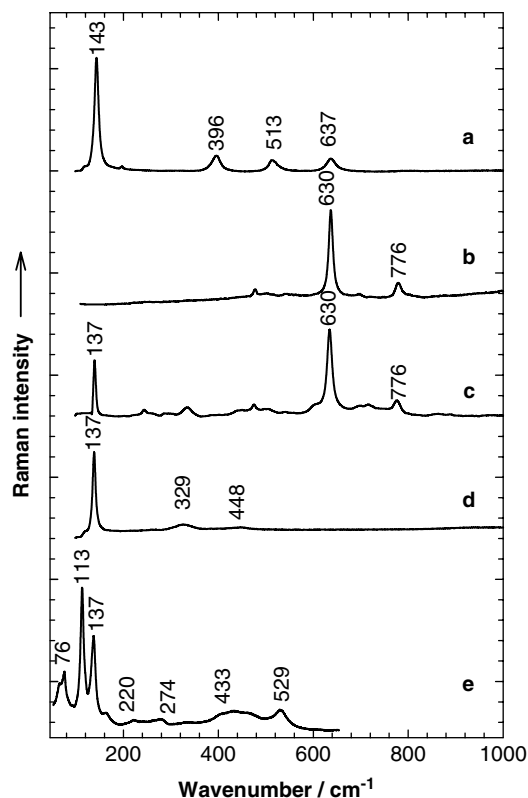


**Figure 4.** Raman spectra of pigments/opacifiers: (a) TiO<sub>2</sub> anatase, (b) cassiterite (c) cassiterite and lead tin yellow type II (d) Lead tin yellow type II (e) lead tin yellow type II and red lead.

was identified on the yellow and green beads (Fig. 4(c) and (d)).<sup>24</sup> Lead-tin oxides have been employed since antiquity as a yellow pigment and opacifier.<sup>25</sup> In Table 3 the Pb/Sn ratio for each colour bead is given. In conjunction with Table 1 the variation in the ratio of lead tin yellow type II and cassiterite to obtain a large variation in colours and opacity can be deduced. CuO (1.04 wt%) and ZnO (0.13 wt%) were added to the basic yellow glass recipe to obtain the green colour, while the turquoise colour was obtained by adding CuO (1.25 wt%), a small presentation of lead tin yellow type II and cassiterite as opacifier. Copper in its oxidized state (Cu<sup>2+</sup>) is responsible for a fine turquoise-blue (for glazes/glasses with sodium and potassium as main fluxing ions<sup>23</sup>) or green (in transparent lead, lime and lime-alkali glazes/glasses<sup>23</sup>) colour in glasses and as it completely dissolves in the melt it cannot be observed with Raman spectroscopy. The combination of Cu (blue for the sodium-potassium-calcium glass) and lead tin yellow type II to obtain a green colour has also been observed in green glass beads excavated in Sri Lanka.<sup>18</sup>

In the spectrum of the orange bead, Raman bands originating from lead tin yellow type II can also be distinguished, but in addition a very strong signal at 113 cm<sup>-1</sup> and a peak at 529 cm<sup>-1</sup> are observed (Fig. 4(e)). In Table 3 it can be seen that, in comparison with the yellow glass, the lead:tin ratio for the orange glass is higher,

**Table 3.** Lead: tin ratio

Sample	Pb	Sn	Pb/Sn
Black	0.1	–	–
Green	7.3	1.9	3.8
Yellow	6.4	1.3	4.9
Plum	0.4	0.1	4
Cobalt blue	–	–	–
Turquoise	0.8	2.0	0.4
Orange	8.8	1.7	5.2

and as the extra peaks occur at wavenumbers very near to that of red lead oxide, it can be deduced that it was incorporated into the lead tin yellow pigment to modify the colour to orange. A similar spectrum has previously been reported in Islamic ceramics from Dugga in Ifriqiya, one sample dating from the 11–12th century (Ziridos period), the other from the 17–18th century (Ottoman period).<sup>26</sup> Furthermore, in Table 1 it can be seen that Zn has been added to the pigment mixture of the orange beads. In a collection of 18–19th century *anime* (semi-finished glass used as opacifier-colourant in other transparent glasses) recipe collections from the Darduin family, Murano, Italy, the addition of zinc to lead-antimonate-tin yellow pigments to obtain the required shade of yellow or orange in glass has been documented. In reconstruction experiments of some of these recipes (potter's yellow type II) it was noted that red Pb<sub>3</sub>O<sub>4</sub> forms as by-product when burnt lead, antimony oxide and ZnO are used as ingredients.<sup>27,28</sup>

BaO and MnO are also present in the yellow and orange beads and were added intentionally, as it is not present in the basic glass of the other colour beads or related to the presence of Sn, Mn, Zn or Pb. Mn is known to act as a decolorant for iron impurities and it is most likely that it was added for this purpose. In modern glass, Ba lowers the melting temperature and decreases the tendency towards devitrification, but it is not known if this was the reason for its inclusion in this glass.

The dark blue beads are coloured with cobalt, which has been in use since antiquity to colour Roman and Egyptian glass (from cobalt containing alum/natron from the western oases of Egypt<sup>29</sup>). A deep blue colour is obtained with 0.2% cobalt or even less. Cobalt is a rare element in the earth's crust and up to the 12th century A.D. the export of cobalt pigments could be related to only two production regions, namely Qamsar and Anarak in Persia and the Erzgebirge Mountains in Saxony, which were geologically rich enough to support, for long periods of time, a trade route over Europe, North Africa and the East as far as China. In both these regions the cobalt is associated with arsenic.<sup>30,31</sup> The cobalt ore in Germany is associated with Ag-bearing minerals and Ni, Bi, Zn or Mo are usually present. Recently, it has been shown that early primary glass production (high Al, high Ca glass) took place at Ile-Ife in southwestern Nigeria

and utilized cobalt associated with high levels of manganese to manufacture dark blue beads.<sup>32</sup>

The cobalt ore, imported from Iran, used in the famous Jingdezhen (China) blue-and-white ware during the 14th to early 15th centuries was rich in iron (Fe : Co = 3:1) and sometimes contained arsenic, nickel and copper.<sup>23</sup> In the 15th century, cobalt ore rich in manganese was discovered in southern China and replaced the imported product.<sup>23</sup>

It has been shown that the cobalt ore used in Vietnam over a long period of time was associated with Mn, and in a large study of more than 550 glass samples from sites from Afghanistan, Pakistan, India, Sri Lanka, Thailand, Malaysia, Indonesia, Vietnam and Cambodia, it was found that all the cobalt blue beads examined contained cobalt associated with large quantities of Mn.<sup>33–36</sup>

The cobalt used to colour the Mapungubwe cobalt blue beads is associated with arsenic and iron (Table 1). The Fe : Co (iron concentration obtained by subtracting the mean value of Fe concentration of the basic glass batch) ratio matches the 3 : 1 ratio obtained in early Chinese ware and the  $\text{As}_2\text{O}_3/\text{CoO}$  weight ratio of  $\sim 1.24$  indicates that the Co : As ratio in the chemical formula of the ore was probably 1 : 1 (some arsenic evaporates during the glass-making process).<sup>31</sup> The absence of Mn makes it unlikely that the cobalt beads originated from the above-mentioned sites around the Indian Ocean or southwestern Nigeria and the absence of Bi, Ni and Mo might also be an indication that the ore originates from Iran rather than Europe. However, large variations in the concentrations of elements in natural ore do occur.

Most ancient glasses and medieval glasses that do not contain any deliberately added colourant have a 'natural' green colour owing to iron as contaminant in the raw materials from which the glass was made.<sup>37</sup> Manganese was added to ancient glasses to remove the green colour caused by iron impurities through reduction, and an excess of manganese results in plum-coloured glass ( $\text{Mn}^{3+}$ ). In the case of the plum-coloured Mapungubwe oblate beads, Mn as well as a small amount of lead tin yellow type II (perhaps to enhance the colour or contamination) was detected (Table 1).

Iron has previously been identified as the pigment in the black beads excavated at Mapungubwe, but the iron content of the Mapungubwe oblates (1.5%) is not enough to obtain a black colour in the form of the reduced iron oxide FeO. At least 6% iron oxide is necessary to colour the glass black and the 1.5% iron oxide combined with 0.2%  $\text{TiO}_2$  (Table 1) would result in the typical greens of Chinese celadon glazes.<sup>23</sup> Raman spectra recorded (532 nm excitation) on black Mapungubwe oblate beads are shown in Fig. 5. Figure 5(a) is the characteristic spectrum of carbon, with the broad D and G bands centered at  $\sim 1300$  and  $\sim 1600 \text{ cm}^{-1}$ . Prominent peaks in the low wavenumber region dominate the bands originating from the glass in the other spectra in Fig. 5. The two sharp peaks at  $330$  and  $357 \text{ cm}^{-1}$  have the appearance of a crystalline phase and occur very near the peaks of pyrite ( $\text{FeS}_2$ ) at  $351$ ,  $386$  and  $443 \text{ cm}^{-1}$ ,

which could have been used as pigment.<sup>38</sup> According to the XRF results in Table 1, the iron concentration in the black beads does not differ from that of the other beads, but the sulfur concentration is higher. It is therefore more likely that sulfur was added to the basic glass recipe to form the Fe-S chromophore traditionally used to produce amber glass and which in sufficiently high concentrations appears black.

During the cooling of a soda-lime-silica glass melt containing iron oxides and sulfur species, ferrous iron ( $\text{Fe}^{2+}$ ) reacts with sulfite ( $\text{SO}_3^{2-}$ ) causing increases in the  $\text{Fe}^{3+}$  (ferric ion) and  $\text{S}^{2-}$  (sulfide) concentrations, which are required for the formation of a chromophore based on  $\text{Fe}^{3+} - \text{S}^{2-} - 3\text{O}^{2-} - n\text{Na}^+$  complexes in the silicate glass. The amber colour intensity of the chromophore depends strongly on the melting temperature, the alkali concentration in the glass, the total iron concentration of the melt and the oxidation state of the melt, which has to be reducing to form<sup>39,40</sup>  $\text{S}^{2-}$ . Except for the amber chromophore containing ferric iron in tetrahedral co-ordination with three oxygens and one sulfur, other iron-sulfur species that occur in the melt are ferrous iron in octahedral co-ordination with oxygen, ferric ion in tetrahedral co-ordination with oxygen, sulfur as sulfate and sulfur as sulfide but not in association with iron.<sup>39,40</sup> This large variation of structures and the resultant environments of the chromophore are probably responsible for the large variation in the Raman spectra (Fig. 5(b–e)). Carbon is usually added as reducing agent to produce modern amber glass and it could have been the case here as well (Fig. 5(a)) or carbon could have been the pigment and the formation of the Fe-S chromophore fortuitous.

Furthermore, the Raman peaks occur at more or less the same wavenumbers ( $290$ ,  $320$ ,  $344$ ,  $370$  and  $400 \text{ cm}^{-1}$ ) as

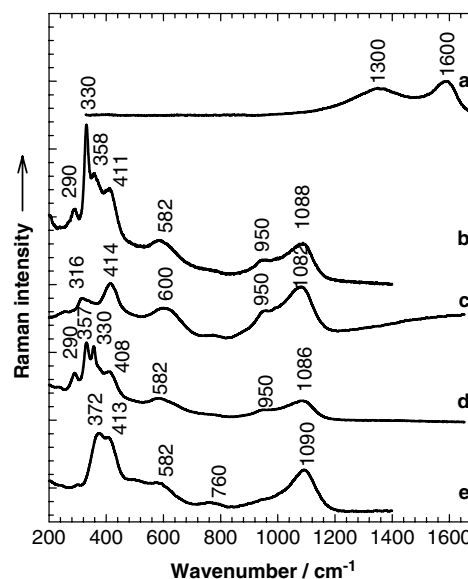


**Figure 5.** Raman spectra recorded on the black glass (a) amorphous carbon; (b), (c), (d) and (e) pigment in black glass recorded on different positions.

Fe-S stretching bands originating from [2Fe-2S] clusters in proteins, which vary in intensity and position with the wavelength of the exciting laser.<sup>41</sup> Resonance effects have also been observed in other pyrite structures such as IrS<sub>2</sub> and MgS.<sup>42,43</sup>

It is quite interesting to note that it was recently reported that although some black Bird Star beads (produced in South or Southeast Asia, 4–9th c.) are coloured with Mn, some are suspected to be coloured with an iron-sulfur combination.<sup>44</sup>

### The larger black beads

The Raman spectra of the larger black beads (Fig. 1(b)) are compared to that of a black Mapungubwe oblate in Fig. 6. As it has previously been suggested that the black beads could have been made at factories around the Indian Ocean, the spectra of two samples from famous glass-making sites (Arikamedu, India and Giribawa, Sri Lanka), are also included. It is clear that the spectra of the two larger black beads are different from that of the Mapungubwe oblate but very similar to that of the Indian and Sri Lankan beads. At a first glance the spectra appear to be of a glass with very high polymerization index ( $I_p = 1.7$ ), but comparison with the spectra in Fig. 5 of the black pigment in the Mapungubwe oblate glass indicates that the peak at  $\sim 415\text{ cm}^{-1}$  may also originate from the Fe-S chromophore. This was confirmed by recording spectra with different exciting wavelengths on the cylindrical black bead (Fig. 7). The shift of the strong  $415\text{ cm}^{-1}$  peak (532 nm laser line, 200 s accumulation time) to  $365\text{ cm}^{-1}$  with a sharp decrease in intensity in the spectrum recorded with the red laser line (1000 s accumulation time) clearly shows that the peaks are resonance-enhanced in the blue-green part of the spectrum.

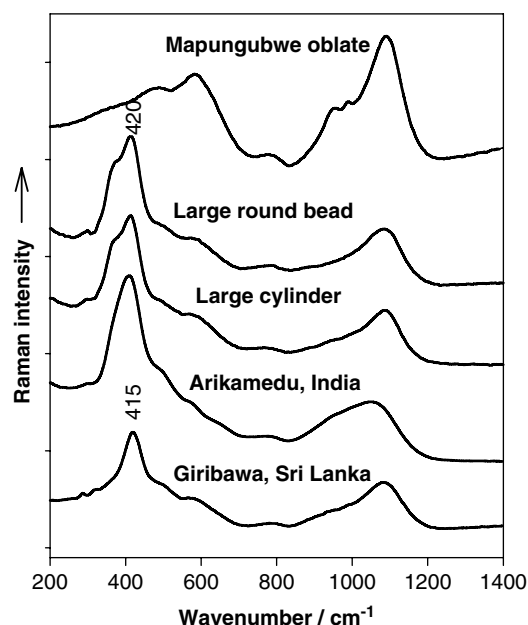


**Figure 6.** Raman spectra of the different black glass beads in comparison with black glass from Arikamedu (India) and Giribawa (Sri Lanka).

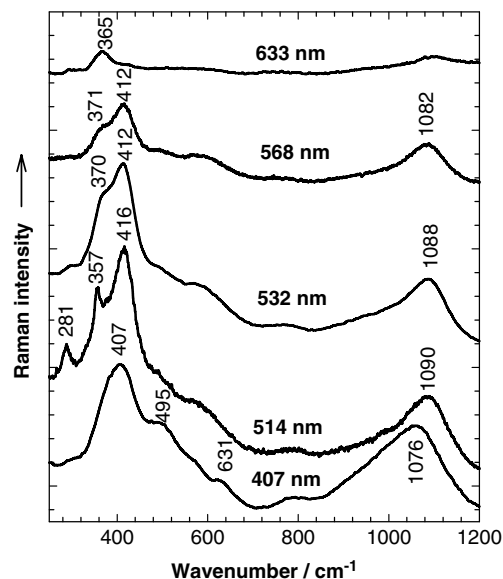


**Figure 7.** Raman spectra recorded on the cylindrical black bead with different exciting laser lines (633, 514, 568, 532 and 407 nm).

In contrast to the Mapungubwe oblates, in which the spectrum varied according to the position probed on the sample (Fig. 5), it was not possible to record spectra from these beads in which the strong resonance peak is absent. This can perhaps be ascribed to higher iron concentrations in the larger beads (Table 4), as well as differences in composition of the fluxing ions.

The main elements (wt%) present in the glass of the specific beads used for the Raman analyses (obtained with EDX measurements) are given in Table 4 and it is clear that three different glass recipes were used to manufacture the beads. In Fig. 8 this is graphically illustrated and the relative

**Table 4.** EDX analysis of main elements in the black beads, as well as corroded Mapungubwe oblate

Element (wt%)	Mapungubwe oblate	Mapungubwe oblate (corroded)	Cylindrical bead	Large round bead
Na	7.32	0.94	13.92	0.53
Mg	0.6	0.74	0.51	0.43
Al	7.26	9.57	6.99	8.0
Si	60.38	63.88	55.64	59.53
P	0.74	1.61	0	0
Cl	3.91	0.53	4.92	2.83
K	8.57	4.22	9.1	15.82
Ca	5.42	10.84	3.18	5.13
Ti	0.74	1.18	0.58	0.82
Fe	3.89	4.89	5.15	6.01
Pb	0.52	0.0	0.0	0.9
Mn	0.1	0.0	0	0



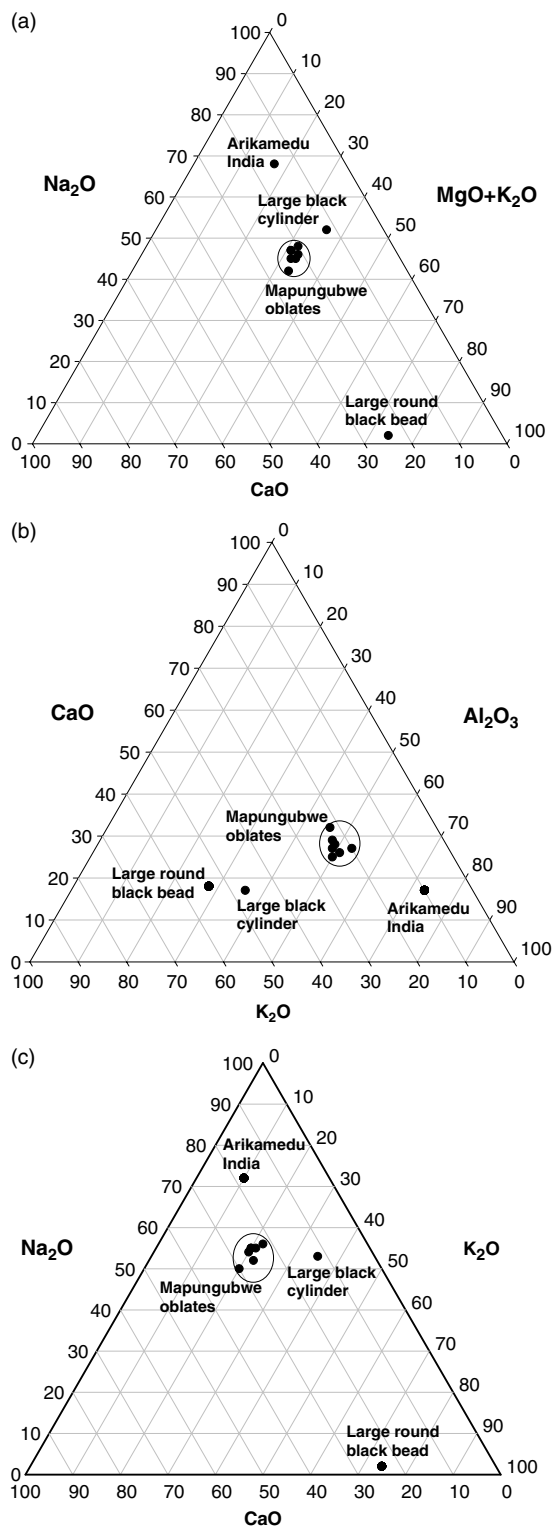


**Figure 8.** Comparison of relative concentrations of ions of the beads in this study: (a) CaO, (MgO + K<sub>2</sub>O) and Na<sub>2</sub>O; (b) K<sub>2</sub>O, Al<sub>2</sub>O<sub>3</sub> and CaO; (c) CaO, K<sub>2</sub>O and Na<sub>2</sub>O.

concentrations of the fluxing ions are also compared to those of the beads from Arikamedu (compositional analysis of

the beads from Giribawa were not available). (It should be noted that three different analysis techniques have been used: XRF for Mapungubwe oblates, SEM-EDX for larger black beads and LA-ICP-MS for the Arikamedu bead. The techniques all have different detection limits and sampling sizes and interpretation of data should be seen in this light.) In all three graphs the Mapungubwe oblates form a separate group and it can be presumed that the black beads originated from three different sites. The beads selected for analysis have been chosen on the basis of physical appearance and therefore do not exclude the possibility that there may be even more chemical variations among similar looking beads. Comparing these diagrams to similar ones in Ref. 34, it becomes clear that the glass composition closely resembles that of beads excavated in Bara, Pakistan (1 B.C.), as well as some other sites around the Indian Ocean.<sup>33–36</sup>

EDX measurements are not sensitive enough to quantify the wt% of the light carbon and oxygen atoms, but a visual comparison between the data shows that there is relatively more carbon and oxygen present in the large cylindrical bead than in the large round or Mapungubwe oblate beads. Furthermore, the FTIR spectra (Fig. 9) of the Mapungubwe beads show that water (bands at 3370 and 1640 cm<sup>-1</sup>) is present in the glass of the cylindrical beads, but absent from the round and Mapungubwe oblate beads. This information might contribute to tracing the origin of the beads.

**White corrosion**

All the previous studies on the glass beads from Mapungubwe commented on the large number of black glass beads that displayed signs of corrosion (Fig. 1(c)). In some instances

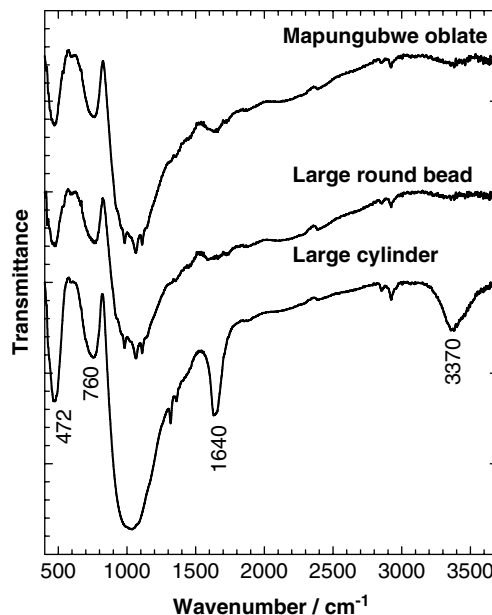


**Figure 9.** (a) FTIR spectra of the three different types of black glass beads excavated at Mapungubwe.

beads are uniformly white or yellow on the outside, but still black inside (Fig. 10).

Raman spectra of pristine glass (black) of the cylindrical and large round beads are compared to that of the corroded part of the bead (white) in Fig. 11(a). The difference between the spectra is obvious, and the disappearance of the peak at  $950\text{ cm}^{-1}$  in the spectra of the white glass is in accordance with the depletion of Na and K ions. The absence of the peak attributed to the Fe-S chromophore is an indication that either sulfur or iron is absent in the corroded glass.

In Fig. 11(b) the Raman spectra of pristine and corroded black glass of a Mapungubwe oblate are compared. The  $I_p$  value has increased to 1.7, an indication of a highly

polymerized network, the centre of gravity of the envelope arising from the Si–O bending modes having shifted downwards to  $482\text{ cm}^{-1}$ , which is near that of pure silica glass and similar to that previously observed in highly corroded museum glass.<sup>21</sup> Table 4 shows the depletion of the sodium and potassium ion concentration as expected in corroded glass.

It has been shown that glasses high in fluxing agents ( $\text{Na}_2\text{O}$ ,  $\text{K}_2\text{O}$ ) and low in stabilizing ions (Ca, Mg) are more prone to corrosion than those in which this ratio is reversed, but for the Mapungubwe oblates the relative ratios of these ions are approximately the same for all the colours. The corrosion is also detected on all three types of beads with different compositions as far as the fluxing ions are concerned.

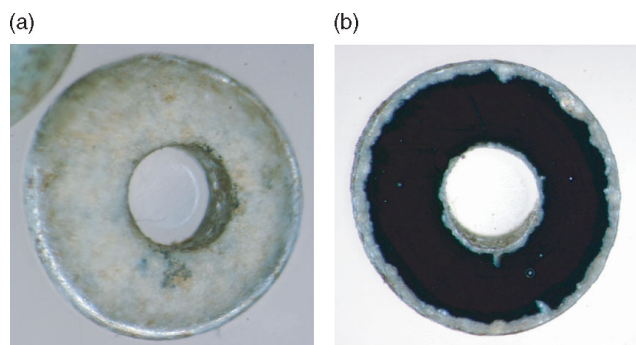


**Figure 10.** Black bead appearing white due to corrosion. (a) Cross-section of the same bead.

### Organic phase detected on most beads

An organic phase was detected on most beads excavated in the grave area and could have originated from a lubricant of the grass roots used to string the beads or could also have been applied during funerary rites. The archives of the bead collection do not have any record of any cleaning or waxing agents that were used to clean the beads after excavation, so it is presumed that the owners of the beads applied the organic phase.

From the Raman spectrum (Fig. 12) it is clear that a C=O bond and an aromatic C=C are present. In industrial

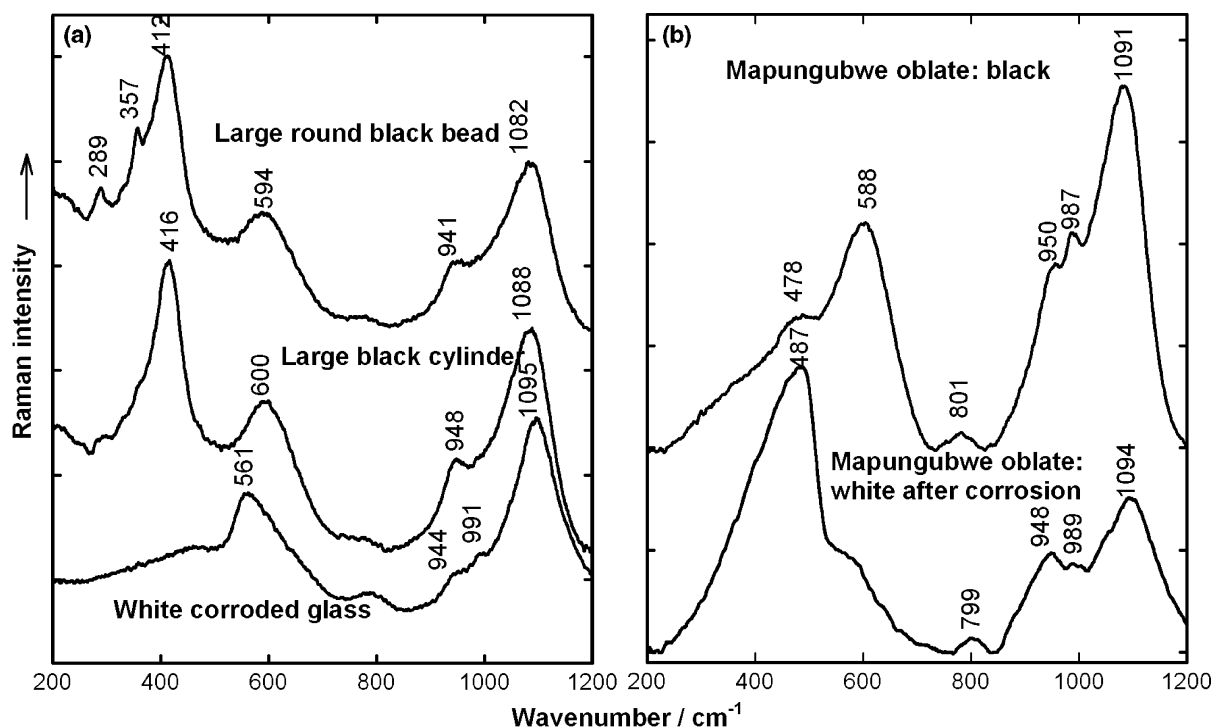


**Figure 11.** (a) Comparison of Raman spectra recorded on the black part of the cylindrical and large round bead with a spectrum recorded on the white glass (large cylinder) and (b) comparison of Raman spectra recorded on the black part of a Mapungubwe oblate with a spectrum recorded on white glass of the same bead.

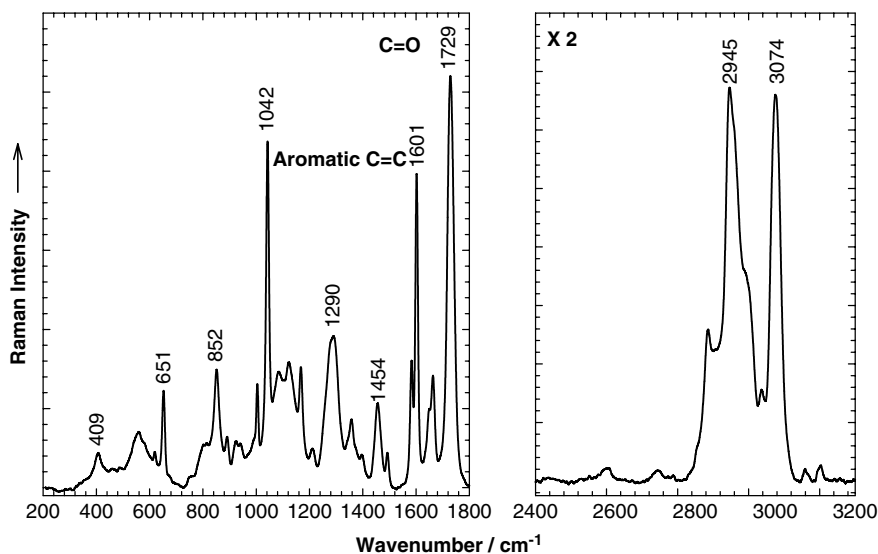


**Figure 12.** Raman spectrum of the organic phase detected on most beads from the 'royal burials'.

pyrite flotation processes, this is characteristic of some collectors, which through chemisorption or through electrostatic interaction influence the surface chemistry. This could have promoted the preferential depletion of sulfur ions leading to the discolouration of the black beads and the amber colour where the corrosion process has not been completed.

## CONCLUSIONS

Using Raman spectroscopy and supportive techniques we have determined a profile of the glass technology used to produce the Mapungubwe oblates. We have shown that there are a number of characteristics of the beads that may eventually help to determine their provenance.

In the first place, although soda/lime/potash glass was produced throughout the ancient world, the high aluminium content eliminates many production centres such as a glass-making factory in Amsterdam, to which many of the trade beads to the North American Indians have been traced, and medieval Venice (9–13th c.).<sup>45–46</sup> Furthermore, the beads used in Refs. 10 and 11 to claim Fustat (old Cairo) as the origin of the Mapungubwe beads (according to a Ce-depleted rare earth element pattern (REE)) also do not have the same basic glass composition as the Mapungubwe oblates.

Second, the pigment palette is quite specific and can also contribute to establishing the provenance of the beads. The cobalt, associated with arsenic, eliminates all sources where cobalt associated with large quantities of manganese were used such as the beads studied in Refs. 32–34.

Considering both the nature of the glass (related to Omeyyad glass) and the pigments used (cobalt associated with arsenic, orange/yellow pigments), it would seem that there is some relationship to Mediterranean/Islamic production technologies, although it has not been possible to find an exact fit with the data currently available to us.

The unique Raman spectra of the pigment in the orange coloured beads, as well as the resonance Raman spectra of the Fe-S chromophore in the black beads, are exceptional tools to identify similar technologies. In combination with the composition of the basic glass recipe used, it should be possible to make a positive identification of glass from possible production sites, which exhibits all the same parameters, as the origin of the beads. This information would make an invaluable contribution towards the understanding of trade routes through and around Africa.

## Acknowledgements

The authors thank B. Gratuze (CNRS-IRAMAT, Orléans) and Laure Dussubieux (The Field Museum of Natural History, Chicago) for valuable discussions and the use of their reference samples. From the University of Pretoria we thank Dr Alan Carr (Department of Physics) for the photograph, Maggi Loubser (XRF and XRD Laboratory) for XRF, Andre Botha (Electronmicroscopy Unit) for the EDX measurements and Me. Sian Tiley of the Mapungubwe Museum for the loan of the beads and for the request of an export permit (No.80/06/06/004/52) from the South African Heritage Resources Agency on our behalf. From the Laboratoire Dynamique, Interactions et Réactivité (LADIR), Paris, we thank Me. Aurelie Tournie for help in recording and analysing some spectra. The financial assistance of the NRF and CNRS towards this research is hereby acknowledged.

## REFERENCES

1. Prinsloo LC, Wood N, Loubser M, Verryrn SMC, Tiley S. *J. Raman Spectrosc.* 2005; **36**: 806.
2. Fouche L. *Mapungubwe: Ancient Bantu Civilization on the Limpopo*. Cambridge University Press: Cambridge, 1937; 1.
3. Chittick HN. *Manda, Excavations at an Island Port on the Kenya Coast, The British Institute in Eastern Africa, Memoir 9*. University Press Oxford: Oxford, UK, 1984; 65.
4. Beck HC. Appendix in *The Zimbabwe Culture: Ruins and Reactions*, Caton-Thompson G (ed). Frank Cass: London, 1971; 185.
5. Beck HC. The beads of the Mapungubwe district. In *Mapungubwe*, Fouché L (ed). Cambridge University Press: Cambridge, 1937; 104.

6. Gardner GA. *Mapungubwe II*. J. L. van Schaik: Pretoria, 1963; 32.
7. Van Riet Lowe C. *The Glass Beads of Mapungubwe*, *Archaeological Series No. 9*, Union of South Africa: Archaeological Survey, Pretoria, 1955.
8. Van der Sleen WGN. *Man* 1956; **56**: 27.
9. Davison CC, Clark JD. *Azania* 1974; **9**: 75.
10. Saitowitz SJ. Glass Beads as Indicators of Contact and Trade in Southern Africa ca. AD 900-AD 1250, Unpublished PhD Thesis, University of Cape Town, Cape Town, 1996.
11. Saitowitz SJ, Reid DL, Van der Merwe NJ. *S. Afr. J. Sci.* 1996; **92**: 101.
12. Wood M. In *The South African Archaeological Society Goodwin Series*, vol. 8, Leslie M, Maggs T (ed), The Society: Cape Town, 2000; 78.
13. Wood M. *Glass Beads and Pre-European Trade in the Shashe-Limpopo Region*, Unpublished MSc Thesis, University of the Witwatersrand, Johannesburg, 2005.
14. Robertshaw P, Glascock MD, Wood M, Popelka RS. *J. Afr. Archaeol.* 2003; **1**: 59.
15. Colomban Ph, March G, Mazerolles L, Karmous T, Ayed N, Ennabli A, Slim H. *J. Raman Spectrosc.* 2003; **34**: 205.
16. Colomban Ph, Milande V, Lucas H. *J. Raman Spectrosc.* 2004; **35**: 68.
17. Colomban Ph, Tournie A, Bellot-Gurlet L. *J. Raman Spectrosc.* 2006; **37**(8): 841.
18. Welter N, Schüssler U, Kiefer W. *J. Raman Spectrosc.* 2007; **38**(1): 113.
19. Colomban Ph, Etcheverry M, Asquier M, Bounichou M, Tournie A. *J. Raman Spectrosc.* 2006; **37**(5): 614.
20. Robinet L, Couptry C, Eremin K, Hall C. *J. Raman Spectrosc.* 2006; **37**: 789.
21. Robinet L, Couptry C, Eremin K, Hall C. *J. Raman Spectrosc.* 2006; **37**: 1278.
22. Carabatos-Nédelec C. Raman scattering of glass. In *Handbook of Raman Spectroscopy: From the Research Laboratory to the Process Line*, Lewis IR, Edwards HGM (ed). Marcel Dekker: New York, 2001; 423.
23. Wood N. *Chinese Glazes*. A & C Black: London, 1999; 63.
24. Clark RJH, Cridland L, Kariuki BM, Harris KDM, Withnall R. *J. Chem. Soc., Dalton Trans.* 1995; **16**: 2577.
25. Biek L, Bayley J. *World Archaeol.* 1979; **2**(1): 1.
26. Colomban Ph, Sagon G, Louchi A, Binous H, Ayed N. *Rev. Archeom.* 2001; **25**: 104.
27. Sandalinas C, Ruiz-Moreno S, López-Gil A, Miralles J. *J. Raman Spectrosc.* 2006; **37**: 1146.
28. Dik J, Hermes E, Peschar R, Schenk H. *Archaeometry* 2005; **47**(3): 593.
29. Shortland AJ, Tite MS, Ewart I. *Archaeometry* 2006; **48**: 153.
30. Gratuze B, Soulier I, Barrandon JN, Foy D. *Rev. Archéom.* 1992; **16**: 97.
31. Zuchchiatti A, Bouquillon A, Katona I, D'Alessandro A. *Archaeometry* 2006; **48**: 131.
32. Lankton JW, Akin Ige O, Rehren T. *J. Afr. Archaeol.* 2006; **4**(1): 111.
33. Colomban Ph, Sagon G, Huy LQ, Liem NQ, Mazerolles L. *Archaeometry* 2004; **46**(1): 125.
34. Dussubieux L. *L'apport de l'ablation laser couplée à l'ICP-MS à la caractérisation des verres: application à l'étude du verre archéologique de l'Océan Indien*, Unpublished PhD Thesis, Université d'Orléans, Orléans, 2001.
35. Dussubieux L, Gratuze B. *Rev. Archéom.* 2003; **27**: 67.
36. Lankton JW, Dussubieux L. *J. Glass Stud.* 2006; **48**: 121.
37. Schreurs JWH, Brill RH. *Archaeometry* 1984; **26**(2): 199.
38. Ushioda S. *Solid State Commun.* 1972; **10**: 307.
39. Beerkens RGC. *Glass Sci. Technol.* 2003; **76**(4): 166.
40. Beerkens RGC, Kahl K. *Phys. Chem. Glasses* 2002; **43**(4): 189.
41. Fu W, Drodzdzewski PM, Davies MD, Sligar SG, Johnson MK. *J. Biol. Chem.* 1992; **267**(22): 15502.
42. Sourisseau C, Cavagnat R, Fouassier M, Jobic S, Deniard P, Brec R, Rouxel J. *J. Solid State Chem.* 1991; **91**: 153.
43. Wolverson D, Bradford C, Prior KA, Cavenett BC. *Phys. Stat. Sol. (b)* 2002; **229**(1): 93.
44. Lankton JW, Dussubieux L, Rehren Th. A study of mid-first millennium CE Southeast Asian specialized glass beadmaking traditions. *Proceedings of the 10th International Conference of the European Society of Southeast Asian Archaeologists*, September, 2004, London, 2006.
45. Karklins K, Hancock RGV, Baart J, Sempowski ML, Moreau JF, Barham D, Aufreite S, Kenyan I. *Archaeometry* 2001; **43**(4): 503.
46. Verità M, Renier R, Zecchin S. *J. Cult. Herit.* 2002; **3**: 261.